# *LINEAR METHOD FOR THE DESIGN OF SHELL AND TUBE HEAT EXCHANGERS INCLUDING SIMPLE FOULING MODELING*

*Julia Coelho Lemos[†], André Luiz Hemerly Costa[†] and Miguel J. Bagajewicz[‡]**

[†] Instituto de Química, Universidade do Estado do Rio de Janeiro, Rio de Janeiro, RJ, Brasil.

[‡]School of Chemical, Biological and Materials Engineering, University of Oklahoma, Norman, Oklahoma USA 73019

***CORRESPONDING AUTHOR:*** *Miguel Bagajewicz. E-mail address: bagajewicz@ou.edu

***KEYWORDS:*** Heat Exchanger Design, Linear Optimization. Fouling

# *ABSTRACT*

Typical heat exchanger design procedures are mostly based on trial and verification (not even trial and error sometimes). They are also based on the use of fixed values of fouling factors, mostly and loosely based on estimates coming from practice and sometimes not even considering values that lead to the usual overdesign that is customary. In this article, we extend a recent globally optimal MILP formulation for the design of shell and Tube heat exchangers (Gonçalves et al., 2016a,b). Our extension leads to an MILP model and consists on adding velocity dependent fouling factors. We also explore the effect of the choice of fouling factors.

# *Introduction*

Heat exchanger design is a very important problem in industries. The classical way of solving it is by trial and verification procedures, as in Kern (1950), where one first guesses the overall heat transfer coefficient, then chooses the heat exchanger geometry according to the required area and then recalculates the overall heat transfer coefficient. If the value found is larger than the one guessed, than the exchanger design is complete; if not, a new value for the overall heat transfer coefficient must be guessed and the procedure must be repeated. These trial procedures are still presented in more recent books (Serth, 2007, Bell, 2008 and Cao, 2010).

Departing from trial and verification or trial and error procedures, there are many works that explore the heat exchanger design as a mathematical optimization problem using MINLP models (Mizutani et al., 2003; Taborek, 2008; Ponce-Ortega et al., 2006 etc.). However, those models are nonconvex and therefore do not guarantee to find the global optimum. Recently, Gonçalves et al. (2016a,b) proposed a MILP model to solve the design problem; because it is linear, it guarantees global optimality.

The majority of the aforementioned procedures consider constant fouling factors for the design, which in some cases may lead to bad designed heat exchangers that will not fulfill their objective correctly. We therefore turn our attention to this issue: Butterworth (2002) analyzed how fouling depends on local temperatures and velocity and how it affects the exchanger design. He does that using a “design-envelope”, which consists of plotting the curves that represent heat transfer and pressure drop on a graph of number of tubes verses tube length. The “design-envelope” is the area above these two curves (Figure 1).

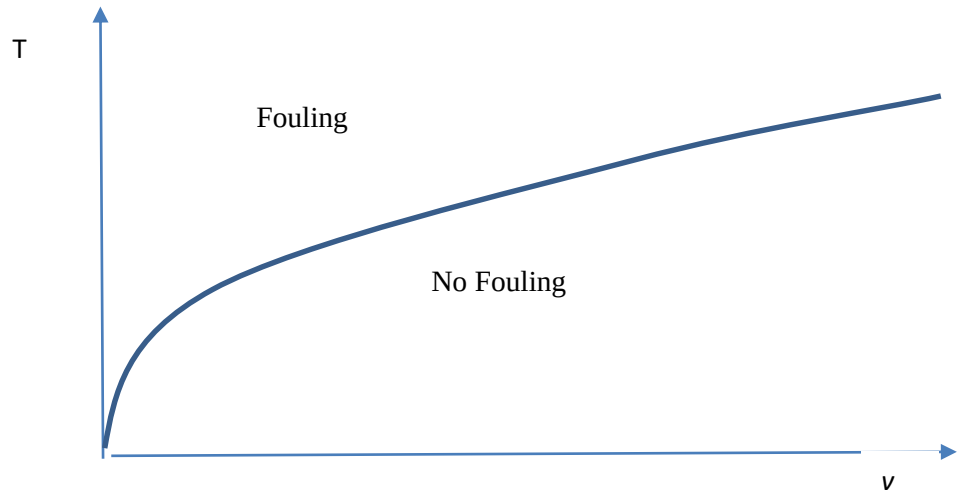


**Figure 1**: Design envelope.

The method was illustrated using many different cases, varying from a no fouling case to cases where the fouling depends on velocity and temperature (Ebert and Panchal, 1997).

Polley et al. (2002) showed how the threshold fouling model can be inserted in the Poddar plot (Poddar and Polley, 2000), which is a graphic procedure similar to the one described by Butterworth (2002). They also discuss how fouling can be mitigated during the design procedure by changing the thermal contact arrangement, increasing the tube-side velocity and/or decreasing the shell-side heat transfer coefficient. They use three examples to illustrate the difference between using constant fouling factors and the fouling threshold: the first example uses the fouling threshold model in the no fouling region; the second and third examples use constant fouling factors varying the number of tube passes. The results for the first example were superior to the other two, showing the disadvantages of using constant fouling factors in the heat exchanger design.

Polley et al. (2011) discussed the design of heat exchangers to achieve an operating period in a refinery preheat train. They propose a procedure to design the heat exchanger for the clean condition and afterwards increase its size to be able to achieve the needed heat load during the entire operating period, while considering a fouling model to predict the fouling factor. They discuss that even with the procedure there is a risk of needing unscheduled cleanings, this risk decreases with the increase of the exchanger size. They also discuss the use of tube inserts and uncertainties.

Shilling (2012) discussed that the margins used in classical heat exchanger design may result in the following problems: unnecessary capital cost, designs with lower velocities and excessive heating of the cold stream or cooling of the hot stream. He resumed the existing "margin methods" and propose a new one that considers a resistance factor.

In this article we extend the linear model presented by Gonçalves et al (2016a,b) to design heat exchangers, which uses fixed fouling factors. Because this model is linear, the results are globally optimal. We show that the results of using fixed values of fouling factors, like those suggested by TEMA or others, can lead to significant area discrepancies when compared to results obtained using a model that actually calculates these fouling factors based on fluid properties and geometric parameters. We then show that when the value of the fouling factor is chosen based on velocities, a possible iterative procedure can be tried. Finally, we introduce the proposed changes in the linear model presented by Gonçalves et al. (2016a,b) to consider the dependency of fouling on the velocity of the fluid and build the appropriate non-iterative robust model.

The article is organized as follows: For completion, we first present the non-linear MINLP model we are using followed by a brief discussion on fouling models. The development of the model based on the one presented by Gonçalves et al (2016a,b),

including the model where fouling factors can be modeled as a function of velocity and keeping the model linear. We then show all the equations for the MILP model proposed in the previous topic. We show results for different cases, including the one of the aforementioned iterative procedure and compare it with the correct solution.

# *Heat Exchanger Model*

We consider heat exchangers with single shell and E-shell type processing fluids that do not go into phase change. We assume that the flow regime is turbulent, which is the most common in industry. We used the Kern model equations (Kern, 1950) and the Dittus-Boelter as well as the Darcy-Weisbach (Saunders, 1988; Incropera, 2006) equations for the calculations of heat transfer coefficients and pressure drop. Fluid allocation is considered to be a parameter, which is determined prior the optimization by the designer. Finally, the problem parameters, which are fixed prior the optimization, are represented using the symbol "^" on top.

We now present all the equations as presented by Gonçalves et al (2016) without any explanations, these equations will serve as base to the development of the MILP model that will be shown later.

***Shell-Side Thermal and Hydraulic Equations***

The Nusselt number for shell-side is given by (Kern, 1950):

$$Nus = 0.36\, Res^{0.55} \widehat{Prs}^{1/3} \quad (1)$$

where $\widehat{Prs}$ is the dimensionless group Prandtl and *Res* is the Reynolds number. The Nusselt number and the Reynolds number are defined as:

$$Nus = \frac{hs\ Deq}{\widehat{ks}} \tag{2}$$

$$Res = \frac{Deq\ vs\ \widehat{\rho s}}{\widehat{\mu s}} \tag{3}$$

where $\widehat{ks}, \widehat{\rho s}$ and $\widehat{\mu s}$ are the thermal conductivity, the density and the viscosity of the fluid, respectively. Regarding the variables, *hs* is the convective heat transfer coefficient, *Deq* is the equivalent diameter and *vs* is the flow velocity.

The equivalent diameter is a function of the outer tube diameter (*dte*) and the tube pitch (*ltp*), and also depends on the layout of the heat exchanger.

$$Deq = \frac{4\ ltp^2}{\pi\ dte} - dte \quad \text{(Square pattern)} \tag{4}$$

$$Deq = \frac{3.46\ ltp^2}{\pi\ dte} - dte \quad \text{(Triangular pattern)} \tag{5}$$

The flow velocity is given by:

$$vs = \frac{\widehat{ms}}{\widehat{\rho s}\ Ar} \tag{6}$$

where $\widehat{ms}$ is the shell-side stream flow rate and *Ar* is the area between adjacent baffles, and can be described by:

$$Ar = Ds\ FAR\ lbc \tag{7}$$

where *Ds* is the shell diameter, *lbc* is the baffle spacing and *FAR* is the free area ratio, that is given by:

$$FAR = \frac{(ltp - dte)}{ltp} = 1 - \frac{dte}{ltp} = 1 - \frac{1}{rp} \tag{8}$$

The pressure drop in the shell-side flow *ΔPs*, not considering nozzle pressure drop, can be described by the next equation (Kern, 1950). Where *fs* is the shell-side friction

factor and *Nb* is the number of baffles that depends on the length of the heat exchanger (L). The equations that describe the friction factor and the number of baffles are also shown below:

$$\frac{\Delta Ps}{\widehat{\rho s}\ \hat{g}} = fs \frac{Ds(Nb+1)}{Deq}\left(\frac{vs^2}{2\ \hat{g}}\right) \tag{9}$$

$$fs = 1.728\ Res^{-0.188} \tag{10}$$

$$Nb = \frac{L}{lbc} - 1 \tag{11}$$

***Tube-Side Thermal and Hydraulic Equations***

The tube-side Nusselt number (*Nut*) is given by the Dittus-Boelter correlation (Incropera, 2006):

$$Nut = 0.023\ Ret^{0.8}\widehat{Prt}^{n} \tag{12}$$

$$Nut = \frac{ht\ dti}{\widehat{kt}} \tag{13}$$

where the parameter *n* is equal to 0.3 for cooling services and 0.4 for heating services. The Reynolds number is given by:

$$Ret = \frac{dti\ vt\ \widehat{\rho t}}{\widehat{\mu t}} \tag{14}$$

where the parameters $\widehat{\mu t}$ and $\widehat{\rho t}$ are the viscosity and the density of the tube-side fluid, respectively. The variable *dti* is the tube inner diameter and *vt* is the tube-side flow velocity:

$$vt = \frac{4\ \widehat{mt}}{Ntp\ \pi\ \widehat{\rho t}\ dti^2} \tag{15}$$

where $\widehat{mt}$ is the flow rate and *Ntp* is the number of tubes per pass.

The pressure drop in the tube-side flow ($\Delta Pt$), considering constant physical properties, is given by (Saunders, 1988):

$$\frac{\Delta Pt}{\widehat{\rho t}\ \hat{g}} = \frac{ft\ Npt\ L\ vt^2}{2\ \hat{g}\ dti} + \frac{K\ Npt\ vt^2}{2\ \hat{g}} \tag{16}$$

where $ft$ is the tube-side friction factor. This equation considers the head loss in the tube bundle, first term in the right hand side, and the head loss in the front and rear headers, second term. The parameter *K* is determined by the number of tube passes and is equal to 0.9 for one tube pass and 1.6 for two or more.

The Darcy friction factor for turbulent flow is (Saunders, 1988):

$$ft = 0.014 + \frac{1.056}{Ret^{0.42}} \tag{17}$$

***Overall Heat Transfer Coefficient***

The expression of the overall heat transfer coefficient (*U*) is:

$$U = \frac{1}{\frac{dte}{dti\ ht} + \frac{\widehat{Rft}\ dte}{dti} + \frac{dte \ln(\frac{dte}{dti})}{2\ \widehat{ktube}} + \widehat{Rfs} + \frac{1}{hs}} \tag{18}$$

where $\widehat{Rft}$ and $\widehat{Rfs}$ are the fouling factors of the tube-side and shell-side streams, respectively and $\widehat{ktube}$ is the thermal conductivity of the tube wall.

***Heat Transfer Rate Equation***

The LMTD method is based on a logarithmic mean temperature ($\widehat{\Delta Tlm}$) described by:

$$\widehat{\Delta Tlm} = \frac{(\widehat{Thi} - \widehat{Tco}) - (\widehat{Tho} - \widehat{Tci})}{\ln\left(\frac{(\widehat{Thi} - \widehat{Tco})}{(\widehat{Tho} - \widehat{Tci})}\right)} \tag{19}$$

The heat transfer rate equation is given by:

$$\hat{Q} = UA\ \widehat{\Delta Tlm}\ \ F \tag{20}$$

where $\hat{Q}$ is the heat load, $A$ is the area and $F$ is the LMTD correction factor.

This correction factor is equal to 1 if the heat exchanger has only one pass, otherwise it is described by the following equation:

$$F\ = \frac{(\hat{R}^2 + 1)^{0.5}\ \ln\left(\frac{(1-\hat{P})}{(1-\hat{R}\,\hat{P})}\right)}{(\hat{R}-1)\ln\left(\frac{2-\hat{P}\left(\hat{R}+1-(\hat{R}^2+1)^{0.5}\right)}{2-\hat{P}\left(\hat{R}+1+(\hat{R}^2+1)^{0.5}\right)}\right)} \tag{21}$$

where:

$$\hat{R} = \frac{\widehat{Thi} - \widehat{Tho}}{\widehat{Tco} - \widehat{Tci}} \tag{22}$$

$$\hat{P} = \frac{\widehat{Tco} - \widehat{Tci}}{\widehat{Thi} - \widehat{Tci}} \tag{23}$$

The heat transfer area ($A$) is given by:

$$A = \ Ntt\ \ \pi\ dte\ L \tag{24}$$

where $Ntt$ is the total number of tubes.

***Bounds on Pressure Drops, Flow Velocities and Reynolds Numbers:***

The variables considered have reference values as lower and upper bounds, that should be taken into the model though the following equation:

$$\Delta Ps \leq \widehat{\Delta Psdisp} \tag{25}$$

$$\Delta Pt \leq \widehat{\Delta Ptdisp} \tag{26}$$

$$\widehat{vsmax} \geq vs \geq \widehat{vsmin} \tag{27}$$

$$\widehat{vtmax} \geq vt \geq \widehat{vtmin} \tag{28}$$

The convective heat transfer coefficient correlations have same parameters that depend on the Reynolds number. As these parameters were fixed previously, we must add bounds on the Reynolds numbers in the shell-side and tube-side:

$$Res \geq 2{\cdot}10^3 \tag{29}$$

$$Ret \geq 10^4 \tag{30}$$

***Geometric Constraints:***

The baffle spacing must be limited between 20% and 100% of the shell diameter (Taborek, 2008a):

$$lbc \geq 0.2\ Ds \tag{31}$$

$$lbc \leq 1.0\ Ds \tag{32}$$

The ratio between the tube length and shell diameter must be between 3 and 15 (Taborek, 2008b):

$$L \geq 3\ Ds \tag{33}$$

$$L \leq 15\ Ds \tag{34}$$

Usually, but not necessarily always, the designer seeks to minimize the heat transfer area (A), which has a direct impact in the exchanger cost.

# *Fouling Models*

Fouling is a very important aspect that has a direct impact on the heat exchanger performance; therefore, it should not be neglected in the heat exchanger design. To be able to include its impact on an exchanger model, one should know how fouling behaves and which variables may influence it in the particular service chosen.

Many works focus on fouling behavior, trying to achieve a fouling model that describes how the fouling resistance varies with time, fluid properties, temperature and fluid-dynamic conditions. These models vary from simple linear models to complex ones like the Ebert and Panchal model (Ebert and Panchal, 1997) that are reviewed by Wilson et al. (2015).

The Ebert and Panchal model represents the dynamics of fouling, but does not provide the final value at infinite time. In this article, we use a simpler model, reported by Nesta and Bennett (2005) where the fouling resistance can be described as a function of velocity:

$$Rft = \widehat{kRft}\ (vt)^{-\alpha Rft} \tag{35}$$

where $\widehat{kRft}$ and $\widehat{\alpha Rft}$ are the parameters of the model. We assume this is the steady state value.

Nesta and Bennett (2005) have only used this model for the tube-side. In this work we make the assumption that equation (35) can be used for both sides of the heat exchanger, based on Caputo et al. (2011).

# *MILP Model*

The MILP model that will be developed here is an adaptation of the one proposed by Gonçalves et al. (2016b). Because the heat exchanger design uses discrete geometrical variables, the discretization of these variables allow the exchanger design problem to be a MILP model. The modification comes from including the fouling model in the MILP model.

The discrete geometric variables and the representation of the list of possible values for each one of them are inner and outer tube diameters ($\widehat{pdti}$ and $\widehat{pdte}$), shell diameter ($\widehat{pDs}$), number of tube passes ($\widehat{pNpt}$), pitch ratio ($\widehat{prp}$), layout ($\widehat{play}$), tube length ($\widehat{pL}$) and number of baffles ($\widehat{pNb}$). The constraints that represent each one of these geometric variables are displayed in equations

$$dte = \sum_{sd=1}^{sdmax} \widehat{ppdte}_{sd}\, yd_{sd} \quad (36)$$

$$dti = \sum_{sd=1}^{sdmax} \widehat{ppdti}_{sd}\, yd_{sd} \quad (37)$$

$$Ds = \sum_{sDs=1}^{sDsmax} \widehat{ppDs}_{sDs}\, yDs_{sDs} \quad (38)$$

$$lay = \sum_{slay=1}^{slaymax} \widehat{pplay}_{slay}\, ylay_{slay} \quad (39)$$

$$Npt = \sum_{sNpt=1}^{sNptmax} \widehat{ppNpt}_{sNpt}\, yNpt_{sNpt} \quad (360)$$

$$rp = \sum_{srp=1}^{srpmax} \widehat{pprp}_{srp} yrp_{srp} \quad (41)$$

$$L = \sum_{sL=1}^{sLmax} \widehat{ppL}_{sL}\, yL_{sL} \quad (42)$$

$$Nb = \sum_{sNb=1}^{sNbmax} \widehat{ppNb}_{sNb}\, yNb_{sNb} \quad (43)$$

The binary variables, represented by *y*, in equations (36) - (43), must obey equations (44) - (50) to map only one geometry for the heat exchanger.

$$\sum_{sd=1}^{sdmax} yd_{sd} = 1 \quad (44)$$

$$\sum_{sDs=1}^{sDsmax} yDs_{sDs} = 1 \quad (45)$$

$$\sum_{slay=1}^{slaymax} ylay_{slay} = 1 \quad (46)$$

$$\sum_{sNpt=1}^{sNptmax} yNpt_{sNpt} = 1 \quad (47)$$

$$\sum_{srp=1}^{srpmax} yrp_{srp} = 1 \quad (48)$$

$$\sum_{sL=1}^{sLmax} yL_{sL} = 1 \quad (49)$$

$$\sum_{sNb=1}^{sNbmax} yNb_{sNb} = 1 \quad (50)$$

As shown by Gonçalves et al. (2016b), to solve the problem faster, one can consider only one set of binary variables, the discrete geometric variables are all represented by this unique set,a multi-index binary variable, where *srow* = (*sd, sDs, slay, sNpt, srp, sL, sNb*) . The new parameters that will represent the commercial values of the geometric variables will be:

$$\widehat{Pdte}_{srow} = \widehat{pdte}_{sd} \quad (51)$$

$$\widehat{Pdt\imath}_{srow} = \widehat{pdt\imath}_{sd} \quad (52)$$

$$\widehat{PDs}_{srow} = \widehat{pDs}_{sDs} \quad (53)$$

$$\widehat{Play}_{srow} = \widehat{play}_{slay} \quad (54)$$

$$\widehat{PNpt}_{srow} = \widehat{pNpt}_{sNpt} \quad (55)$$

$$\widehat{Prp}_{srsrow} = \widehat{prp}_{srp} \quad (56)$$

$$\widehat{PL}_{srow} = \widehat{pL}_{sL} \quad (57)$$

$$\widehat{PNb}_{srow} = \widehat{pNb}_{sNb} \quad (58)$$

Therefore, instead of having equations (36) – (50), the geometric variables will be represented by the following equations:

$$dte = \sum_{srow} \widehat{Pdte}_{srow}\, yrow_{srow} \tag{59}$$

$$dti = \sum_{srow} \widehat{Pdti}_{srow}\, yrow_{srow} \tag{60}$$

$$Ds = \sum_{srow} \widehat{PDs}_{srow}\, yrow_{srow} \tag{61}$$

$$lay = \sum_{srow} \widehat{Play}_{srow}\, yrow_{srow} \tag{62}$$

$$Npt = \sum_{srow} \widehat{PNpt}_{srow}\, yrow_{srow} \tag{63}$$

$$rp = \sum_{srow} \widehat{Prp}_{srow} yrow_{srow} \tag{64}$$

$$L = \sum_{srow} \widehat{PL}_{srow}\, yrow_{srow} \tag{65}$$

$$Nb = \sum_{srow} \widehat{PNb}_{srow}\, yrow_{srow} \tag{66}$$

$$\sum_{srow} yrow_{srow} = 1 \tag{67}$$

The idea of Gonçalves et al. (2016b) is to substitute the linear equations (59) – (67) into the heat exchanger model, making the necessary arrangements to have a linear model linear. In this topic we only show the equations that are the starting point of our changes, the remaining model equations can be found in Gonçalves et al. (2016b).

The velocity equations are:

$$vs = \frac{\widehat{ms}}{\widehat{\rho s}} \sum_{srow} \frac{\left(\widehat{PNb}_{srow}+1\right)}{\widehat{PDs}_{srow}\widehat{PFAR}_{srow}\widehat{PL}_{srow}}\, yrow_{srow} \tag{68}$$

$$vt = \frac{4\,\widehat{mt}}{\pi\,\widehat{\rho t}} \sum_{srow} \frac{\widehat{PNpt}_{srow}}{\widehat{PNtt}_{srow}\widehat{Pdti}_{srow}{}^{2}}\, yrow_{srow} \tag{69}$$

For equation (20) the equivalent linear equation based on fixed values of fouling factors is:

$$\hat{Q}\left(\sum_{srow}\frac{\widehat{pdte}_{srow}}{\widehat{pht}_{srow}\,\widehat{pdti}_{srow}}yrow_{srow}+\widehat{Rft}\sum_{srow}\frac{\widehat{pdte}_{srow}}{\widehat{pdti}_{srow}}yrow_{srow}+\right.$$

$$\left.\frac{\sum_{srow}\widehat{pdte}_{srow}\,yrow_{srow}\ln\left(\frac{\widehat{pdte}_{srow}}{\widehat{pdti}_{srow}}\right)}{2\,\widehat{Ktube}}+\widehat{Rfs}+\sum_{srow}\frac{1}{\widehat{phs}_{srow}}yrow_{srow}\right)\leq$$

$$\left(\frac{100}{100+\widehat{Aexc}}\right)\left(\pi\sum_{srow}\widehat{pNtt}_{srow}\,\widehat{pdte}_{srow}\,\widehat{pL}_{srow}yrow_{srow}\right)\cdot\widehat{\Delta Tlm}\;\hat{F}_{srow} \qquad (70)$$

The fouling factor expressions, after the velocity equations have been substituted and further linearized are:

$$Rfs=\widehat{kRfs}\left(\frac{\widehat{ms}}{\widehat{\rho s}}\sum_{srow}\frac{\left(\widehat{PNb}_{srow}+1\right)}{\widehat{PDs}_{srow}\widehat{PFAR}_{srow}\widehat{PL}_{srow}}\right)^{-\widehat{\alpha Rfs}}yrow_{srow} \qquad (71)$$

$$Rft=\widehat{kRft}\left(\frac{4\,\widehat{mt}}{\pi\,\widehat{\rho t}}\sum_{srow}\frac{\widehat{PNpt}_{srow}}{\widehat{PNtt}_{srow}\widehat{Pdti}_{srow}{}^{2}}\right)^{-\widehat{\alpha Rft}}yrow_{srow} \qquad (72)$$

Once equations (71) and (72) are inserted in equation (70), we get the following heat transfer rate equation:

$$\hat{Q}\left(\sum_{srow}\frac{\widehat{pdte}_{srow}}{\widehat{pht}_{srow}\,\widehat{pdti}_{srow}}yrow_{srow}+\right.$$

$$\widehat{kRft}\left(\frac{4\,\widehat{mt}}{\pi\,\widehat{\rho t}}\right)^{-\widehat{\alpha Rft}}\sum_{srow}\left(\frac{\widehat{PNpt}_{srow}}{\widehat{PNtt}_{srow}\widehat{Pdti}_{srow}{}^{2}}\right)^{-\widehat{\alpha Rft}}\frac{\widehat{pdte}_{srow}}{\widehat{pdti}_{srow}}yrow_{srow}+$$

$$\frac{\sum_{srow}\widehat{pdte}_{srow}\,yrow_{srow}\ln\left(\frac{\widehat{pdte}_{srow}}{\widehat{pdti}_{srow}}\right)}{2\,\widehat{Ktube}}+$$

$$\left.\widehat{kRfs}\left(\frac{\widehat{ms}}{\widehat{\rho s}}\sum_{srow}\frac{\left(\widehat{PNb}_{srow}+1\right)}{\widehat{PDs}_{srow}\widehat{PFAR}_{srow}\widehat{PL}_{srow}}\right)^{-\widehat{\alpha Rfs}}yrow_{srow}+\right.$$

$$\sum_{srow} \frac{1}{\widehat{phs}_{srow}} yrow_{srow} \Bigg) \leq$$

$$\left(\frac{100}{100+\widehat{Aexc}}\right) \left( \pi \sum_{srow} \widehat{pNtt}_{srow} \widehat{pdte}_{srow} \widehat{pL}_{srow} yrow_{srow} \right) \cdot \widehat{\Delta Tlm} \ \widehat{F}_{srow} \qquad (73)$$

In the next section we present the results for solving the MILP problem in four different ways. The first two ones will consider the fouling resistance constant and equal to the worst and best scenarios that correspond to finding the maximum and minimum values for equation (41), for both sides of the heat exchanger. In the third case, we consider the iterative procedure that can be applied to the MILP model, we use two different starting points: maximum and minimum fouling resistances. And finally, we solve the problem using the MILP model proposed in this article, that includes fouling model into the design problem.

# *Example 1*

In this example, we consider that the fluid flowing on both sides of the heat exchanger is water, and the cold fluid is in the tubes. Table 1 presents its physical properties and Table 2 the characteristics of the heat exchanger.

**Table 1** – Water physical properties

| Density (kg/m$^3$) | Viscosity (Pa s) | Conductivity (W/mK) | Heat capacity (J/kgK) | Prandtl |
|---|---|---|---|---|
| **1000** | 0.000695 | 0.628 | 4178 | 4.624 |

**Table 2** – Heat exchange characteristics

| Fluid | Cold | Hot |
|---|---|---|
| **Mass flow rate** | 200 | 100 |

| | | |
|---|---|---|
| **Inlet temperature (K)** | 32 | 70 |
| **Outlet temperature (K)** | 40 | 54 |

The values used for the fouling model constants were the ones reported by Nesta and Bennett (2005). These values were considered to be the same for both sides of the heat exchanger, with $\widehat{kRft}$ and $\widehat{kRfs}$ assuming a value of 0.00062, and $\widehat{\alpha Rft}$ and $\widehat{\alpha Rfs}$ assuming a value of 1.65. We consider that the area must be 11% larger than the required area. All the problems were solved using GAMS/CPLEX .

***Case 1:*** The first case considers the fouling resistance constant and its value is calculated prior the optimization using Equation (41) and considering the worst-case scenario (fouling resistance using the lower bound on the velocities). As a result, the fouling resistance on the tube-side is equal to 6.20·10-4 m2K/W and on the shell-side it is 1.90·10-3 m2K/W. We note that trial and verification is not needed here because the MILP model, with constant or velocity dependent equations renders the U and the area simultaneously. If one uses the above calculated fouling factor values the only verification needed is that the fouling factors are smaller than the assumed ones. Otherwise, one can attempt to iterate. The results are presented on table 3, with the area already using the 11% excess:

**Table 3** – Results for case 1

| | | | |
|---|---|---|---|
| **dte (m)** | 0.01905 | **Deq (m)** | 0.01375 |
| **dti (m)** | 0.01575 | **Res** | 11977.91 |
| **L (m)** | 4.8768 | **Nus** | 104.97 |
| **Nb** | 8 | **hs (W/m$^2$K)** | 4794.72 |
| **Npt** | 4 | **vt (m/s)** | 1.229 |
| **rp** | 1.25 | **Ret** | 27861.26 |
| **Ds (m)** | 1.524 | **Nut** | 152.66 |
| **lay** | 2 | **ht (W/m$^2$K)** | 6087.02 |
| **ltp** | 0.02381 | **U (W/m$^2$K)** | 323.27 |
| **Ntt** | 3341.60 | **A (m$^2$)** | 974.80 |
| **Ntp** | 835.40 | **fs** | 0.2957 |
| **ebc** | 0.5419 | **ft** | 0.02835 |

| | | | |
|---|---|---|---|
| **Ar** | 0.1652 | **ΔPs** | 54065.18 |
| **vs (m/s)** | 0.6055 | **ΔPt** | 31370.82 |

To analyze the results obtained and verify if the area found is larger than the area needed, we calculate the fouling resistance with equation (35) applied to both tube and shell sides using the velocity found and recalculate the heat transfer coefficient. The results are in table 4.

**Table 4 –** Recalculation according to the fouling model

| Variable | Calculated value |
|---|---|
| **Rft ($m^2K/W$)** | $4.41 \cdot 10^{-4}$ |
| **Rfs ($m^2K/W$)** | $1.42 \cdot 10^{-3}$ |
| **New U ($W/m^2K$)** | 325.42 |

We can observe that the Rf values obtained in this optimization are smaller than those assumed and therefore, in a trial and verify context, this exchanger is acceptable. The remaining question is if the area is close to a minimum possible value.

***Case 2:*** The second case considers the best-case scenario, using the velocity upper bound to calculate the fouling resistance prior the optimization. The fouling resistance is considered constant and equal to the value calculated through equation (41), with the upper bound velocities. The values calculated are $1{,}01 \cdot 10^{-4}$ $m^2K/W$ in the tube-side and $1{,}97 \cdot 10^{-4}$ $m^2K/W$ in the shell-side. Table 5 presents the results and Table 6 the recalculation using the same procedure as the previous case.

**Table 5** – results for case 2

| | | | |
|---|---|---|---|
| **dte (m)** | 0.01905 | **Deq (m)** | 0.01887 |

| | | | |
|---|---|---|---|
| **dti (m)** | 0.01575 | **Res** | 3098.48 |
| **L (m)** | 3.6585 | **Nus** | 177.05 |
| **Nb** | 6 | **hs (W/m²K)** | 5893.02 |
| **Npt** | 2 | **vt (m/s)** | 2.35 |
| **rp** | 1.25 | **Ret** | 53177.45 |
| **Ds (m)** | 0.8382 | **Nut** | 256.04 |
| **lay** | 1 | **ht (W/m²K)** | 10209.07 |
| **ltp** | 0.02381 | **U (W/m²K)** | 1553.84 |
| **Ntt** | 875.38 | **A (m²)** | 191.57 |
| **Ntp** | 437.69 | **fs** | 0.2473 |
| **ebc** | 0.5226 | **ft** | 0.02494 |
| **Ar** | 0.08761 | **ΔPs** | 50087.65 |
| **vs (m/s)** | 1.141 | **ΔPt** | 40704.42 |

Table 6 – Recalculation according to the fouling model

| Variable | Calculated value |
|---|---|
| Rft ($m^2K/W$) | 1.52·10-4 |
| Rfs ($m^2K/W$) | 4.98·10-4 |
| U ($W/m^2K$) | 1014.24 |

In this case study, the calculated fouling factors are smaller than those used to design the exchanger and a new trial would be needed.

***Case 3:*** In this case we performed an iteration procedure to test if it converges. This procedure consists of solving consecutive optimization problems with fixed fouling resistances, where the fouling resistances of the next problem are calculated prior the optimization through equation (41) using the velocities obtained in the previous iteration.

This case study was solved with three different initial points, in all of them the initial fouling resistance was calculated prior the optimization with equation (41), the difference between them is the velocity value considered. The first initial point calculated considered the velocities lower bounds. The results to each one of the problems solved in the iterative procedure are presented in Table 9.

**Table 7 –** Iterative procedure results (low starting velocities)

| Problem | Rft ($m^2K/W$) | Rfs ($m^2K/W$) | vt (m/s) | vs (m/s) |
|---|---|---|---|---|
| **1** | $6.2 \cdot 10^{-4}$ | $1.9 \cdot 10^{-3}$ | 1.229 | 0.605 |
| **2** | $4.41 \cdot 10^{-4}$ | $1.42 \cdot 10^{-3}$ | 1.665 | 0.605 |
| **3** | $2.67 \cdot 10^{-4}$ | $1.42 \cdot 10^{-3}$ | 1.087 | 0.705 |
| **4** | $5.40 \cdot 10^{-4}$ | $1.10 \cdot 10^{-3}$ | 1.087 | 0.542 |
| **5** | $5.40 \cdot 10^{-4}$ | $1.70 \cdot 10^{-3}$ | 1.420 | 0.605 |
| **6** | $3.48 \cdot 10^{-4}$ | $1.42 \cdot 10^{-3}$ | 1.087 | 0.705 |
| **7** | $5.40 \cdot 10^{-4}$ | $1.10 \cdot 10^{-3}$ | 1.087 | 0.542 |
| **8** | $5.40 \cdot 10^{-4}$ | $1.70 \cdot 10^{-3}$ | 1.420 | 0.605 |
| **9** | $3.48 \cdot 10^{-4}$ | $1.42 \cdot 10^{-3}$ | 1.087 | 0.705 |
| **10** | $5.40 \cdot 10^{-4}$ | $1.10 \cdot 10^{-3}$ | 1.087 | 0.542 |

As we can observe, from problem 4 the results start to repeat in a certain pattern. The loop does not converge. In this case, the iterative procedure, using the maximum fouling resistance as initial point, is not a good option.

The second possibility is to use the mean velocity to calculate the fouling resistance for the initial point. The results are displayed in table 8.

**Table 8 –** Iterative procedure (average starting velocities)

| Problem | Rft ($m^2K/W$) | Rfs ($m^2K/W$) | vt (m/s) | vs (m/s) |
|---|---|---|---|---|
| **1** | $1.97 \cdot 10^{-4}$ | $4.29 \cdot 10^{-4}$ | 1.973 | 0.837 |
| **2** | $2.02 \cdot 10^{-4}$ | $8.31 \cdot 10^{-4}$ | 1.680 | 0.828 |
| **3** | $2.63 \cdot 10^{-4}$ | $8.47 \cdot 10^{-4}$ | 1.616 | 0.698 |
| **4** | $2.80 \cdot 10^{-4}$ | $1.12 \cdot 10^{-3}$ | 1.791 | 0.771 |
| **5** | $2.40 \cdot 10^{-4}$ | $9.50 \cdot 10^{-4}$ | 1.865 | 0.837 |
| **6** | $2.22 \cdot 10^{-4}$ | $8.32 \cdot 10^{-4}$ | 1.680 | 0.828 |
| **7** | $2.63 \cdot 10^{-4}$ | $8.47 \cdot 10^{-4}$ | 1.616 | 0.698 |
| **8** | $2.80 \cdot 10^{-4}$ | $1.12 \cdot 10^{-3}$ | 1.791 | 0.771 |

The results start to repeat in a certain pattern and not converge to any result.

The third and last attempt to converge the iterative procedure is to use the minimum value for the fouling resistance at the initial point; the results are in table 9.

Table 9 – Iterative procedure (maximum starting velocities)

| Problem | Rft ($m^2K/W$) | Rfs ($m^2K/W$) | vt (m/s) | vs (m/s) |
|---|---|---|---|---|
| **1** | $1.01 \cdot 10^{-4}$ | $1.97 \cdot 10^{-4}$ | 2.347 | 1.141 |
| **2** | $1.52 \cdot 10^{-4}$ | $4.98 \cdot 10^{-4}$ | 1.973 | 0.957 |
| **3** | $2.02 \cdot 10^{-4}$ | $6.67 \cdot 10^{-4}$ | 1.902 | 0.801 |
| **4** | $2.15 \cdot 10^{-4}$ | $8.94 \cdot 10^{-4}$ | 1.616 | 0.785 |
| **5** | $2.81 \cdot 10^{-4}$ | $9.24 \cdot 10^{-4}$ | 1.865 | 0.837 |
| **6** | $2.22 \cdot 10^{-4}$ | $8.32 \cdot 10^{-4}$ | 1.680 | 0.828 |
| **7** | $2.63 \cdot 10^{-4}$ | $8.47 \cdot 10^{-4}$ | 1.616 | 0.785 |
| **8** | $2.81 \cdot 10^{-4}$ | $9.24 \cdot 10^{-4}$ | 1.865 | 0.837 |

The results in table 9 show that this attempt to solve the problem through the iterative procedure was not successful either.

The three initial points tried here were not capable of giving a good result in the iterative procedure, for this example. It shows the importance of developing new models that can solve the problem already considering the fouling model.

***Case 4:*** In this case, the developed MILP model was used to find the global optimum for the presented problem. The results are presented at table 10.

Table 10 – results for case 4

| | | | |
|---|---|---|---|
| **dte (m)** | 0.**0254** | **Deq (m)** | 0.**0251**6 |
| **dti (m)** | 0.0221 | **Res** | 33483.62 |
| **L (m)** | 4.8768 | **Nus** | 184.77 |
| **Nb** | 10 | **hs (W/m²K)** | 4612.33 |
| **Npt** | 4 | **vt (m/s)** | 2.0029 |
| **rp** | 1.25 | **Ret** | 63689.62 |
| **Ds (m)** | 1.2192 | **Nut** | 295.79 |
| **lay** | 1 | **ht (W/m²K)** | 8405.19 |
| **ltp** | 0.03175 | **U (W/m²K)** | 757.29 |
| **Ntt** | 1041.78 | **A (m²)** | 405.20 |
| **Ntp** | 260.44 | **fs** | 0.2437 |
| **ebc** | 0.4433 | **ft** | 0.02414 |
| **Ar** | 0.1081 | **ΔPs** | 55584.54 |
| **vs (m/s)** | 0.9250 | **ΔPt** | 55573.61 |

The value found in the present case is 405.20 $m^2$, which represents a gain of 140.6% compared to the value found with fixed fouling resistance, different from this case where the fouling resistance is not a parameter.

# *Conclusions*

The proposed MILP model presented in this article can solve the heat exchanger design problem giving as a result the global optimum. Other forms to solve this problem were tried, in case 1 the area found is larger than the required area, therefore you can design a smaller exchanger that would be better option. In case 2 the exchanger found is too small, and cannot perform the necessary heat exchange. Case 3 was an attempt to find the optimum through an iterative procedure, but for all the three initial points that were used the loop was infinite.

We conclude that the proposed MILP model is a good way of solving the heat exchanger design problem. This model considers fouling and how it is affected by velocity. The majority of works that explore the exchanger design does not focus on the fouling problem.

# *Nomenclature*

*A* - area ($m^2$)

*Ar* - area between adjacent baffles ($m^2$)

*Deq* - equivalent diameter (m)

*Ds* - shell diameter (m)

*dte* - outer tube diameter (m)

*F* - LMTD correction factor

*FAR* - free ratio area

*fs* - Darcy friction factor for shell-side

*ft* - Darcy friction factor for tube-side

*hs* - convective heat transfer coefficient for shell-side ($W/m^2K$)

*ht* - convective heat transfer coefficient for tube-side ($W/m^2K$)

*ks* - thermal conductivity of the fluid on shell-side (W/mK)

*kt* - thermal conductivity of the fluid on tube-side (W/mK)

*L* - length of the heat exchanger (m)

*lbc* - baffle spacing (m)

*ltp* - tube pitch

*lay* - layout of the heat exchanger

*ms* - stream flow rate on shell-side (kg/s)

*mt* - stream flow rate on tube-side (kg/s)

*Nb* - number of baffles

*Npt* - number tube passes

*Ntt* - total number of tubes

*Nus* - Nusselt number for shell-side

*Nut* - Nusselt number for tube-side

*Prs* - Prandtl for shell-side

*Prt* - Prandtl for tube-side

*Q* - heat load (W)

*Res* - Reynolds number for shell side

*Rfs* - fouling factor on shell-side ($m^2K/W$)

*Rft* - fouling factor on tube-side ($m^2K/W$)

*rp* - pitch ratio

*U* - overall heat transfer coefficient

*vs* - flow velocity for shell-side (m/s)

*vs* - flow velocity for tube-side (m/s)

## *Greek*

$\Delta Ps$ - pressure drop on shell-side (Pa)

$\Delta Pt$ - pressure drop on tube-side (Pa)

$\Delta Tlm$ - logarithmic mean temperature (K)

$\mu s$ - viscosity of the fluid on shell-side (Pa.s)

$\mu t$ - viscosity of the fluid on tube-side (Pa.s)

$\rho s$ - density of the fluid on the shell-side (kg/m$^3$)

$\rho t$ - density of the fluid on the tube-side (kg/m$^3$)

# *References*


Butterworth, D. Design of shell-and-tube heat exchangers when the fouling depends on local temperature and velocity. *Applied Thermal Engineering*, v. 22, p. 789-801, 2002.

Cao, E. *Heat Transfer in processing engineering*. McGraw-Hill, New York, 2009.

Caputo, A. C., *et al*. Joint economic optimization of heat exchanger design and maintenance policy. Applied Thermal Engineering, 2011, v. 31, pp. 1381-1392.

Ebert, W., and Panchal, C.B., 1997, Analysis of Exxon crude-oil-slip stream coking. In: *Fouling mitigation of industrial heat exchange equipment*. Begell House, New York, pp. 451-460.

Gonçalves, C.O.; Costa, A. L. H.; Bagajewicz, M.J. Shell and Tube Heat Exchanger Design Using Mixed-Integer Linear Programming, *AIChE Journal*, 2016a.

Incropera, F. P.; De Witt, D. P. *Fundamentals of Heat and Mass Transfer*. John Wiley & Sons, 6$^{th}$ ed., 2006.

Kern, D.Q. *Process Hear Transfer*. McGraw-Hill, New York, 1950.

Mizutani, F. T, *et al.* Mathematical programming model for heat-exchanger network synthesis including detailed heat-exchanger designs. 1. Shell-and-tube heat-exchanger design. *Ind. Eng. Chem Res.*, 2003, v. 42, pp 4009–4018.

Nesta, J. and Bennett, C. A. Reduce fouling in shell-and-tube heat exchangers. *Hydrocarbon Processing*, 2004, pp. 77-82.

Poddar, T. K. and Polley, G. T. Optimize shall-and-tube heat exchanger design. *Chemical Engineering Progress,* September, pp. 41-46.

Polley, G. T., *et al.* Evaluation of laboratory crude oil threshold fouling data for application to refinery pre-heat trains, *Appl. Therm. Eng*., 2002, v. 22, pp. 777-788.

Polley, G. T., *et al*. Design of shell-and-tube heat exchangers to achieve a specified operating period in refinery preheat trains. *Heat Transfer Engineering*, 2011, v. 32, pp. 314-319.

Ponce-Ortega, J. M., *et al.* Minimum-investment design of multiple heat exchangers using a MINLP formulation. *Chem. Eng. Res. Des.*, 2006, v. 82, pp. 905-910.

Saunders, E. A. D. *Heat Exchangers: Selection, Design and Construction*. John Wiley & Sons, New York, 1988.

Schilling, R. L. Fouling and uncertainty margins in tubular heat exchanger desing: an alternative. Heat Transfer Engineering, 2012, v.33, pp. 1094-1104.

Serth, R. W. *Process heat transfer principles and applications*. Elsevier, Oxford, 2007.

Taborek, J. Input Data and Recommended Practices. In: *Heat Exchanger Design Handbook*. Ed. G.F. Hewitt, Begell House, New York, 2008a.

Taborek, J. Performance Evaluation of a Geometry Specified Exchanger. In: *Heat Exchanger Design Handbook*. Ed. G.F. Hewitt, Begell House, New York, 2008b.

Taborek, J. Calculation of Shell-Side Heat Transfer Coefficient and Pressure Drop. In: *Heat Exchanger Design Handbook*. Ed. G.F. Hewitt, Begell House, New York, 2008c.

TEMA. *Standards of the Tubular Exchangers Manufactures Association*. Tubular Exchanger Manufacturers Association, 9th ed., New York, 2007.

Wilson, D. I., Polley, G. T. e Pugh, S. J., 2005, Ten Wears of Ebert, Panchal and the threshold fouling concept. *Proc. 6th Int. Conference on Heat exchanger, Fouling and Cleaning – Challenges and Opportunities*, 2005, Kloster Irsee, Germany, pp. 25-36.